



CONTROLLING OF N-P JUNCTION PROPERTIES

Sanjay M Wagh

Central India Research Institute, 34, Farmland, Ramdaspath, Nagpur 440010, India
waghsm.ngp@gmail.com

ABSTRACT

Characteristics of cylindrical N-P junction are shown to be interestingly different than those of planar N-P junction, thereby permitting better control of its luminescence properties.

Indexing terms/Keywords

N-P junction, cylindrical configuration, control of luminescence

Academic Discipline And Sub-Disciplines

Solid State Physics, Semiconductor Devices

SUBJECT CLASSIFICATION

PACS: 85.30De, 85.30Kk, 85.30Mn

TYPE (METHOD/APPROACH)

Theoretical analysis of cylindrical configuration for N-P junction



Council for Innovative Research

Peer Review Research Publishing System

Journal: INTERNATIONAL JOURNAL OF COMPUTERS & TECHNOLOGY

Vol. 11, No. 3

www.ijctonline.com, editorijctonline@gmail.com

INTRODUCTION

The theory of the *planar N-P junction* is quite well known [1, 2] and characterizes its thickness d as:

$$d = \frac{1}{e} \sqrt{\frac{2\varepsilon(V_J - V_{ext})}{(N_d + N_a)}} \left[\sqrt{\frac{N_a}{N_d}} + \sqrt{\frac{N_d}{N_a}} \right] \quad (1)$$

where N_d is the donor concentration, N_a is the acceptor concentration, ε is the dielectric constant of the material, e is the electronic charge, V_J is the built-in voltage across the junction, and V_{ext} is the applied voltage.

However, alternative configuration geometries for the N-P junction do not appear to have been explored adequately. Of particular interest to us here is a cylindrical configuration for the N-P junction.

CYLINDRICAL GEOMETRY FOR THE N-P JUNCTION

We refer to Figure 1 for notations related to the cylindrical configuration of the N-P junction.

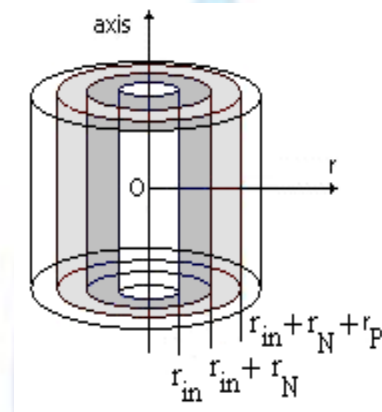


Fig 1: Cylindrical N-P junction

The inner cylinder is taken here to be N-type with dopant concentration of *donors* as N_d , and the outer cylinder to be of P-type with the corresponding dopant concentration of *acceptors* as N_a . An abrupt junction is then assumed to form at the radius $r_{in} + r_N$.

Diffusion of dopants within the N-type region makes positive charges accumulate at the radius r_{in} thereby creating a depletion layer of thickness r_N within the N-type region. On the other hand, the diffusion of dopants within the P-type region produces accumulation of negative charges at the radius $r_{in} + r_N + r_p$. This results in a depletion layer of thickness r_p within the P-type region.

A built-in voltage across radius r_N within the N-type region is denoted by V_N and that across radius r_p within the P-type region is denoted by V_p . The total built-in voltage V_J across the N-P junction, that is, across the N-P junction radius $r_N + r_p$, is:

$$V_J = V_N + V_p \quad (2)$$

The charge neutrality of the junction is:

$$\alpha N_d r_{in} r_N = \beta N_a (r_{in} + r_N) r_p \quad (3)$$

where donor provides α number of elementary charges and acceptor accepts β number of elementary charges.

Defining

$$x = \frac{r_N}{r_{in}}, \quad y = \frac{r_p}{r_{in}}, \quad t = x + y \quad (4)$$



we have

$$\frac{\alpha N_d}{\beta N_a} = \left(\frac{1+x}{x} \right) y \quad (5)$$

In what follows, we work under the approximation

$$x \ll 1, \quad y \ll 1, \quad t \ll 1 \quad (6)$$

which we refer to as a *thin junction*. Notice that

$$r_N = r_P \Rightarrow \alpha N_d \approx \beta N_a \quad (7)$$

That is to say, equal doping concentrations of the two regions lead to equal thicknesses of the depletion layers within the N-type and P-type regions.

Change in the potential energy by total amount is

$$eV_J = e(V_N + V_P) \quad (8)$$

Under equilibrium, the steady-state value of the voltage V_N across the depletion layer within the N-type region is provided by Poisson's equation [1, 2]:

$$\nabla^2 V_N = \frac{e\alpha N_d}{\varepsilon} \quad (9)$$

where ε is the dielectric constant of the base material of the N-P junction.

For cylindrical symmetry under considerations here, Poisson's equation reduces to

$$\frac{d^2 V_N}{dr^2} + \frac{1}{r} \frac{dV_N}{dr} = \frac{e\alpha N_d}{\varepsilon} \quad (10)$$

a purely radial equation.

Uniformly graded N-P junction

For an abrupt N-P junction with *constant* concentrations N_d and N_a , we therefore obtain

$$V_N = \frac{e\alpha N_d}{\varepsilon} r_{in}^2 x^2 \equiv \frac{e\alpha N_d}{4\varepsilon} r_N^2 \quad (11)$$

Similarly, we also obtain:

$$V_P = \frac{e\beta N_a}{\varepsilon} r_{in}^2 y^2 \equiv \frac{e\beta N_a}{4\varepsilon} r_P^2 \quad (12)$$

From Eq. (5), we have:

$$\frac{V_P}{V_N} \approx \frac{\alpha N_d}{\beta N_a} \times \frac{1}{(1+x)^2} \approx \frac{\alpha N_d}{\beta N_a} \quad (13)$$

For the junction thickness, we therefore obtain using Eq. (8):

$$d = \frac{\sqrt{2}}{e} \sqrt{\frac{2\varepsilon(V_J - V_{ext})}{N_a + N_d}} \left[\sqrt{\frac{N_a}{N_d}} + \sqrt{\frac{N_d}{N_a}} \right] \quad (14)$$

Thickness of the cylindrical N-P junction is $\sqrt{2}$ times that of the planar junction, then. Also, for $N_a \gg N_d$, we have:

$$d \approx \frac{2}{\varepsilon} \sqrt{\frac{\varepsilon(V_J - V_{ext})}{N_d}} \quad (15)$$

Capacitance per unit length of the cylindrical junction is:

$$C = \frac{2\pi\epsilon}{\ln(1+t)} \approx \frac{2\pi\epsilon}{t} \approx \frac{2\pi r_{in}\epsilon}{d}, \quad t \ll 1 \tag{16}$$

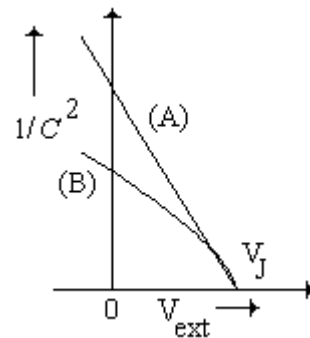


Fig. 2: Capacitance per unit length of the N-P junction

With applied voltage, capacitance per unit length of the junction changes as in curve (A) of Figure 2.. For $N_a \gg N_d$, we then measure V_J and N_d from this plot, likewise to the case of a planar junction.

Radial graded N-P junction

Radial doping gradient may be developed within the cylindrical N-P junction. When the developed doping gradient(s) can be approximated by $N_d \propto N_{d0}r$ and $N_a \propto N_{a0}r$ within the junction, that is, within $r_{in} \leq r \leq r_{in} + r_N + r_P$, then the Poisson equation has solution::

$$V_N = \frac{eN_{d0}}{9\epsilon} r_N^3 \quad \text{and} \quad V_P = \frac{eN_{a0}}{9\epsilon} r_P^3 \tag{17}$$

and the junction thickness is obtained as:

$$d = \left(\frac{9\epsilon(V_J - V_{ext})/e}{(\alpha N_{d0})^2 + (\beta N_{a0})^2} \right)^3 \left[\left(\frac{(\alpha N_{d0})^2}{\beta N_{a0}} \right)^{1/3} + \left(\frac{(\beta N_{a0})^2}{\alpha N_{d0}} \right)^{1/3} \right] \tag{18}$$

Then, for $N_{a0} \gg N_{d0}$, we have

$$d \approx \left(\frac{9\epsilon(V_J - V_{ext})}{e\alpha N_d} \right)^{1/3} \tag{19}$$

The junction capacitance per unit length is then represented by curve (B) of Figure 2.

OTHER FEATURES OF CYLINDRICAL N-P JUNCTION

Electric field across the cylindrical N-P junction under considerations here is:

$$E = \frac{V_T}{r \ln(1+t)} \approx \frac{V_T}{rt} \approx \frac{V_T r_{in}}{rd}, \quad t \ll 1 \tag{20}$$

with $r_{in} \leq r \leq r_{in} + r_N + r_P$. The electric field is maximum at r_{in} as can be expected for a cylindrical capacitor. *Dielectric breakdown* thus occurs first at r_{in} within the junction. The nature of the electric field of the *cylindrical* N-P junction is, interestingly, *different* than that of the planar N-P junction for which it is constant across the junction.

If E_s is the dielectric strength of the base material of the junction, then we have

$$V_b = V_J \left(\frac{E_s}{E_J} - 1 \right) \equiv E_s d - V_J \tag{21}$$



where V_b , the breakdown voltage, is the value of V_{ext} at which the breakdown initiates in the junction and

$$E_J = \frac{V_J r_m}{rd} \quad (22)$$

is intrinsic or the in-built strength of the electric field within the junction.

Now, for the avalanche breakdown, the current I_a is $I_a = mI_s$ where I_s is the reverse bias saturation current and m is the multiplication factor defined by $m = \frac{1}{1 - (V_R/V_B)^n}$ with V_R being the reverse bias voltage and V_B being the breakdown voltage (at which $m \rightarrow \infty$), and the power n being in the range 3-6, usually.

The avalanche breakdown luminescence has the high energy emission spectrum given by

$$U(\nu) = A \left[1 - \operatorname{erf} \left(\frac{h\nu}{\Psi} \right) \right] \text{ with } \Psi = \sqrt{\frac{3\pi}{8}} \left(\frac{\mu E k T_e}{u_s} \right) \quad (23)$$

where A is a constant, μ is the ohmic mobility, E is the electric field, kT_e is the energy of the hot carriers, and u_s is the speed of sound in the base material.

The above features are explorable for cylindrical N-P junction, in details, thus.

DISCUSSION

We have recently shown [3, 4] that the cylindrical geometry of discharge-tube plays an important role in the controlling of the characteristics of the phenomenon of the Joshi effect [5 -11]. Similar control via external illumination by light is of importance for applications of N-P junction properties. Natural issue to investigate was of the role of cylindrical geometry for N-P junction in the case semiconductor hetero-structures. then.

We thus argue here that the occurrence of the dielectric breakdown firstly close to the inner junction radius can permit better controlling of the N-P junction properties than is permissible for its planar configuration. We also note that our considerations are applicable to a doped-nanorod [12 -17].

REFERENCES

- [1] Kittel, C. 1976. Introduction to Solid State Physics, John Wiley, New York.
- [2] Pankove, J. L. 1971. Optical processes in semiconductors, Prentice-Hall, New Jersey.
- [3] Wagh, S. M., Deshpande, D. A. 2011. Revisiting the Joshi Effect, Current Science. 10 November 2011, Vol. 101(9), 1182-1190.
- [4] Wagh, S. M., Deshpande, D. A. 2012, Essentials of Physics, Volume(s) I & II, Prentice-Hall, New Delhi.
- [5] Joshi, S. S., Narasimhan, V. 1940. A Light Effect in Chlorine under Electrical Discharge, Current Science, 9, 535-537.
- [6] Kher, V. G. 1971. Mechanism of a low frequency (10 Hz to 10 kHz) A.C. electrodeless discharge & Joshi effect, Nagpur Univ. J., I, 96-103.
- [7] Kher, V. G., Kelkar, M. G. 1962. High Frequency Electrodeless Discharge & the Effect of Irradiation: Part I - Mechanism of Electrodeless Discharge in Air at Low Pressure, J Sci. Ind. Res., 21B, No. 7, 293-300.
- [8] Kher, V. G., Kelkar, M. G. 1962. High Frequency Electrodeless Discharge & the Effect of Irradiation: Part II - Mechanism of Joshi Effect, J Sci. Ind. Res., 21B, No. 8, 360-366.
- [9] Kher, V. G., Hirade, J. P., Kshirsagar, S. R. 1970. The effect of irradiation on the current pulses in a low-frequency electrodeless argon discharge, J Phys. B: Atom, Molec. Phys., 3, 1539-1543.
- [10] Arnikar, H. J. 1971. Nagpur Univ. J., II, 97-124.
- [11] Arnikar, H. J. 1982. Current Science, 51, 1103-1105.
- [12] Murthy, D.H.K., Xu, T., Chen, W. H., Houtepen, A.J., Savenije, T.J., Siebbeles, L.D.A., Nys, J. P., Krzeminski, C., Grandidier, B., Stievenard, D., Pareige, P., Jomard, F., Patriarche, G., Lebedev, O. I. 2011. Efficient photogeneration of charge carriers in silicon nanowires with a radial doping gradient, arxiv.org/physics/1106.5642.
- [13] Garnett, E. C., Yang, P. D. 2008. Silicon Nanowire Radial p-n Junction Solar Cells, J. Am. Chem. Soc., 130, 9224-9225.
- [14] Kayes, B. M., Atwater, H. A., Lewis, N. S. 2005. Comparison of the device physics principles of planar and radial p-n junction nanorod solar cells, J. Appl. Phys., 97, 114302.



- [15] Garnett, E. C., Tseng, Y-C., Khanal, D. R., Wu, J., Bokor, J., Yang, P. 2010. Dopant profiling and surface analysis of silicon nanowires using capacitance-voltage measurements, *Nature. Nanotechn.*, 4, 311-314.
- [16] Koren, E., Berkovitch, N., Rosenwaks, Y. 2010. Measurement of Active Dopant Distribution and Diffusion in Individual Silicon Nanowires, *NanoLett.*, 10, 1163.
- [17] Perea, D. E., Hemesath, E. R., Schwalbach, E. J., Lensch-Falk, J. L., Voorhes, P. W., Lauhon, L. J. 2009. Direct measurement of dopant distribution in an individual vapour-liquid-solid nanowire, *Nature. Nanotechn.*, 4, 315-319.

Author's biography with Photo



SANJAY M. WAGH, PhD in Physics, is currently professor and director at the Central India Research Institute, Nagpur, India.

In 2007, he discovered a mathematical way of defining Measures over any Category. These works led him to propose the Universal Theory of Relativity, which has “universal” or “absolute” time. In 2009, he proposed that light consists of momentum-less quanta of only energy, and also explained the wave properties of radiation as the wavy fluctuations of the number of quanta resulting from the characteristics of the process of their emission. This emission-mechanism for the wave of quanta then explains the results of Michelson-Morley type experiments without needing “relative” time. Since 2013, he has investigated the acceleration dependence of the Doppler Effect to show that acceleration plays an important role in Doppler shifts of spectral lines of, in particular, astronomical sources.

His research interests include Theoretical Astrophysics, Image Processing, Fundamental Physical Interactions, Nano-scale phenomena, the Joshi effect, Physics of Sports, Category Theory, and Universal Relativity.

